MDPI

Article

Impact of Inline Polyacrylamide Polymer Flocculation on the Mechanical and Hydrological Properties of Saline Tailings

Bob Boshrouyeh [1],*, Mansour Edraki [1], Thomas Baumgartl [2], Allan Costine [3], Sebastian Quintero Olaya [4], Kateřina Lepková [5] and Deepak Dwivedi [5]

[1] Sustainable Minerals Institute, The University of Queensland, St Lucia, QLD 4072, Australia; m.edraki@uq.edu.au

[2] Geotechnical and Hydrogeological Engineering, Federation University, Churchill, VIC 3842, Australia; t.baumgartl@federation.edu.au

[3] CSIRO Mineral Resources, Waterford, WA 6152, Australia; allan.costine@csiro.au

[4] School of Civil Engineering, The University of Queensland, St Lucia, QLD 4072, Australia; s.quintero@uq.edu.au

[5] Curtin Corrosion Centre, WA School of Mines—Minerals, Energy and Chemical Engineering, Faculty of Science and Engineering, Curtin University, Perth, WA 6102, Australia; k.lepkova@curtin.edu.au (K.L.)

* Correspondence: m.boshrouye@student.uq.edu.au

Abstract: This study examines the geotechnical and hydro-mechanical behaviour of a model slurry used in high-solids, high-salinity applications, both before and after inline flocculation with an anionic polyacrylamide. Initial evaluations showed untreated tailings (UT) with a water content of 107%, void ratio of 2.6, and dry density of 0.711 t/m^3, compared to polymer-amended tailings (PAT) with 53% water content, a void ratio of 1.6, and a dry density of 1.069 t/m^3. Post-flocculation consolidometer tests revealed a distinct consolidation mode, with PAT showing 60% less settlement within the first 48 h and achieving 50% more free water drainage. Polymer treatment improved consolidation parameters, yielding a lower compressibility index (Cc of 0.74 vs. 1.05 for raw slurry), a higher coefficient of consolidation (Cv of 0.005 cm^2/s for PAT vs. 0.0009 cm^2/s for raw slurry), and an increased water retention capacity. Additionally, PAT demonstrated a final void ratio of 0.62 compared to 0.51 for the UT sample and an internal porosity characterised by discrete voids, supporting enhanced stability for long-term rehabilitation. These findings underscore the potential of inline flocculation to improve tailings management in saline conditions.

Keywords: inline flocculation; consolidation; settling; hydraulic conductivity; high-solid tailings; dewatering

1. Introduction

Among the several available techniques for treating fine-particle tailings, polymer-bridging flocculation is an effective approach which achieves solid–liquid separation by forming larger aggregated structures with higher settling rates than the individual particles [1–5]. One of the industrially applied methods is in-pipe or inline flocculation, where a polymer is added at high dosages to the thickener underflow, resulting in the additional aggregation and water release on deposition compared to conventional low-solids in-tank thickening processes [6,7]. While this polymer's addition technology has been applied in the minerals and oil sands industries to greatly increase the permeability of tailings and therefore dewatering on deposition, many of the fundamental aspects remain poorly understood [8]. Despite several patents and the strong industry interest (e.g., McColl et al., 2004 [9], Poncet and Gaillard, 2010 [10]), tailings deposited from this process may have properties that are beneficial for rehabilitation, but there is not enough data available on how their properties change over time yet (e.g., consolidation, permeability, void ratio, etc.), particularly under highly saline conditions [11,12].

While previous studies have demonstrated the effectiveness of polymer addition in improving solid–liquid separation and permeability in tailings, there remains a need for the deeper investigation into how inline polymer treatment impacts the long-term consolidation, microstructural stability, and hydraulic properties of tailings, particularly in high-solids and high-salinity contexts [8,9]. Recent advancements in testing systems, such as slurry consolidometers, provide new opportunities to capture the full geotechnical behaviour of polymer-amended tailings. However, few studies have leveraged these technologies to study the unique characteristics of polymer-treated tailings under realistic field-like stress conditions [13,14].

The addition of high dosages of polymer to high-solids tailings streams leads to an effective densification of the aggregate structures with further dewatering achieved compared to traditional techniques [9,15,16]. By implementing this method, the rapid dewatering of tailings can be initiated at or close to the point of deposition. It is important to understand the changes in geotechnical properties of inline flocculated materials, as these parameters impact critical factors like the flow behaviour of tailings and the design and construction of tailings storage facilities (TSFs) [17,18]. The saturated hydraulic conductivity, pore water pressure, water retention capacity, and tensile stress due to desiccation can affect the hydraulic performance of polymer-treated tailings. These parameters also have a significant influence on the mechanical stability, durability and environmental performance of deposited mine tailings [19,20] as well as the future closure of TSFs [21].

It must be pointed out that the polymer-treated tailings compared to the conventional tailings deposits will present potential reclamation advantages such as early consolidation and trafficability, less potential instability of the embankment surfaces, and less supernatant with an overall drier tailings stack [22,23]. Although tailings are site-specific, the reclamation of dewatered high-density tailings is an effective approach in favour of sustainable closure which requires a systematic way to understand all the properties of the deposited materials.

Understanding the sedimentation and consolidation behaviour of tailings is essential in delivering higher performance operations by creating stable tailings dams and also estimating the settlement and the final volume of the materials [24–26]. Qin et al. [27] proposed a simple analytical solution to estimate the settlement and volume variation in tailings deposited in a TSF. The changes in geotechnical properties of tailings during consolidation have been investigated, but the behaviour of aggregates created by in-line flocculation in high-solid/high-salinity applications during settling and consolidation, plus the stability of these new materials, are not yet fully understood [28–31].

Traditional oedometers have limitations in terms of operating mostly for clay-rich tailings [32,33] and extra attention needs to be paid to material responses related to the stress gradient during engineering practices [34,35]. Hence, the use of new testing systems with an increased capability for different types of tailings is becoming more popular. The slurry consolidometer is one such system, offering a promising approach for studying the consolidation behaviour of materials, even those with high water content [13], in the lab under simulated field conditions [14]. This approach allows tailings with different densities to settle before consolidating under various loading cycles, with the capability of recording the properties of the materials with high gravimetric moisture contents and monitoring the changes from a slurry-like to solid-like state. In fact, through slurry consolidation testing, the settling behaviour of mine tailings under consolidation can be evaluated and predicted, which would otherwise take a prohibitively long time through self-consolidation [36,37].

By focusing on these aspects, this study not only enhances our understanding of the underlying mechanisms in polymer-bridging flocculation but also introduces new insights into the consolidation dynamics, stability, and hydraulic conductivity of tailings treated with high-dosage polymers. These findings have potential implications for improving tailings management practices by enabling safer, more stable deposition methods and by supporting the design of TSFs that meet the environmental and regulatory standards for sustainable closure and rehabilitation. This study contributes to the literature by providing

a detailed characterisation of tailings behaviour through synchrotron X-Ray tomography and consolidometer testing, offering a wide-ranging analysis of how polymer-amended tailings perform under operational stresses over time.

This study builds upon previous research [38,39], which examined the interactions of different polymer chemistries with mineral particles in saline, high-solids tailings streams. Those studies highlighted the ionic strength dependence of polymer-tailings interactions, establishing a practical framework for optimising dewatering strategies. Based on those findings, this study applies a targeted high-dosage polymer treatment to evaluate its effects on the geotechnical and hydraulic properties of tailings in a controlled setting. This approach enables a detailed exploration of the effects of polymer-treated tailings on consolidation, drainage, and stability.

The objective of this study was to evaluate the impact of high-dosage polymer addition on geotechnical properties such as settling rate, consolidated density, rate of consolidation, and the hydraulic conductivity of tailings. The initial physical properties of a sample of raw slurry and polymer-treated slurry were evaluated along with their water retention characteristics, while synchrotron-sourced X-Ray tomography provided direct evidence of the changing texture of materials and altered pore size distribution. Experiments were then conducted using a slurry consolidometer for a comprehensive monitoring of the changes in raw and flocculated materials under increasing applied stress.

2. Materials and Methods

2.1. Materials

Kaolinite-NY prestige, silica 200G and silica fine sand were purchased from Sibelco Company (Brisbane, Australia), to prepare the initial slurry. Table 1 lists the dominant minerals for each slurry ingredient in this study. For this study, an acrylamide/acrylate copolymer, BASF's Magnafloc$^®$ 336 (Melbourne, Australia) was selected because its general behaviour is considered representative of nominally equivalent products available from other polymers suppliers. Magnafloc$^®$ 336 is a very high molecular weight anionic polyacrylamide supplied as a free-flowing granular powder. The intrinsic viscosity (IV), as specified by the supplier, was 24 dL/g, providing a relative indication of its solution dimensions. Higher MW polymers typically offer a larger hydrodynamic size of chains in solution, with increasing MW-producing loops and, more importantly, long extended tails that can form bridges with other particles to create aggregates [40]. Under highly saline conditions, as applied in this study, the polymer chains are expected to be more mobile and flexible on the colloidal surface, which allows the restructuring of aggregated clusters to proceed unhindered [41].

Table 1. Synthetic slurry ingredient composition.

	SiO$_2$ (%)	Al$_2$O$_3$ (%)	Fe$_2$O$_3$ (%)	TiO$_2$ (%)
Kaolinite-NY prestige	49.2	35	0.94	0.96
Silica 200G	99.6	0.17	0.02	0.03
Silica fine sand	98.5	0.1	0.3	0.9

A synthetic homogenous tailings slurry was prepared in 0.6 M NaCl solution to avoid the natural variability that exists with real tailings samples and to enable the preparation of large batches for testing. The slurry was prepared at 50 wt% solids from a combination of 25% kaolin, 45% silica 200G (93% finer than 53 μm), and 30% silica fine sand (99% finer than 0.3 mm), as described elsewhere [42]. It was revealed that this combination of the kaolin, silica 200G silt, and silica fine sand produce a slurry that can provide a wide dynamic response in the material behaviour after adding the polymer due to having plastic fine grained particles (25% kaolin in this study) [43]. Moreover, this synthetic material would be assumed to be sensitive to liquefaction-related strength loss, which is consistent with examples of tailings from a variety of mineral types, including iron ore, gold, mineral

sands, and nickel tailings [44]. The specific gravity of the slurry solid particles was 2.64. Conditioning of the slurries was conducted at 1200 rpm for five days in a baffled 200 L tank to ensure a stable, reproducible size for the duration of testing, which was confirmed by laser diffraction measurements.

Working polymer solutions (0.4 wt%) were prepared in the same saline solution used for the slurry make-up. The weighed polymer was added slowly to the vortex produced in salted water under vigorous mixing to fully disperse the powder. Initial strong agitation with an A310 impeller at 250 rpm for 30 min was followed by gentle agitation (80–100 rpm) for 16 h to produce clear, homogenous solutions. Polymer solutions were aged for 3 days in a cool room (4 °C) to ensure optimal activity before adding to the slurry and producing polymer-amended tailings (PAT) [45].

2.2. Inline Polymer Addition

Figure 1 shows the lab-scale experimental set-up used to simulate the inline flocculation process [11,46]. This set-up was developed to assess polymer performance in high-solids tailings applications, addressing limitations found in conventional testing methods (e.g., beakers, plungers, and mechanical devices) which often lead to inconsistent mixing conditions that may not accurately reflect the true effectiveness of the polymers themselves [46]. The main advantage of the low-shear chaotic mixer (or topological mixer) as a laboratory tool is that it gives a uniform shear history across the vessel, in contrast to the distinct zones of shear that will exist in a stirred tank [47]. To control the polymer dosage, the polymer solution (45 mL/min) and slurry (0.25 L/min) were pumped to the inlet of the pre-conditioning coil (1 m length, 7.7 mm I.D.) before entering the chaotic mixer for continued mild mixing. The final mixed product was then collected from the discharge point. All experiments were conducted at room temperature, and the pH was maintained within a neutral range of 6.5–7.5. This controlled environment was selected to ensure consistency and to provide a stable baseline for the analysis of mechanical and hydraulic properties following flocculation.
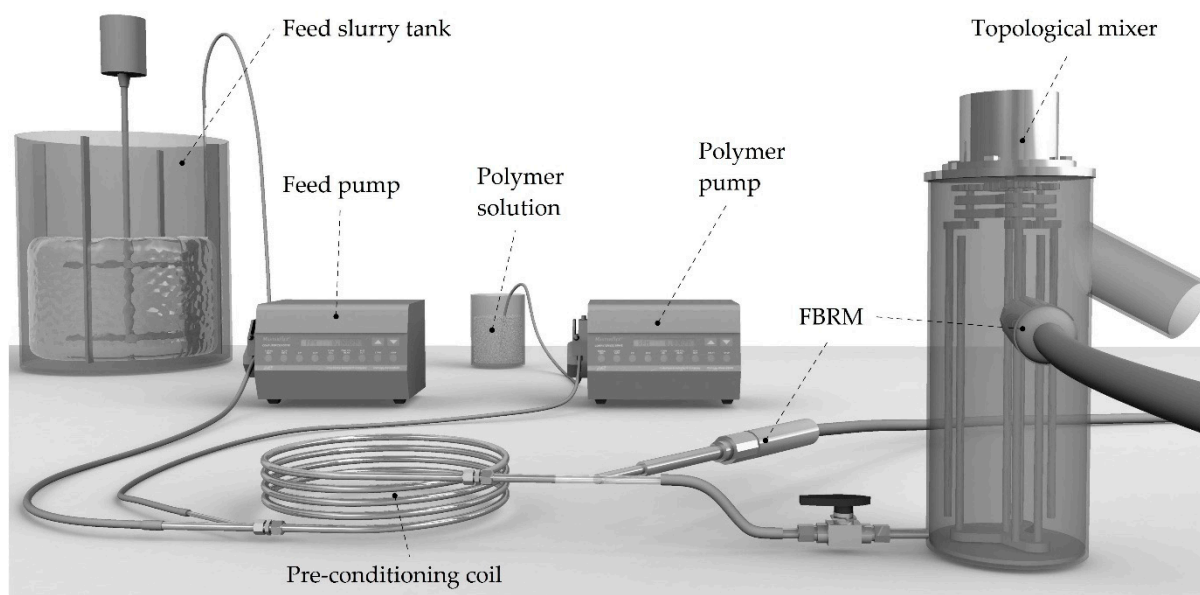

Figure 1. Tapered shear set-up for polymer addition to high-solids suspensions (Note the FBRM was not used in the current study).

The selection of the specific anionic polyacrylamide used in this study was informed by previous studies, where we systematically explored various polymer types [38]. The current study, therefore, represents an application of those foundational findings, focusing

on high-dosage treatments to evaluate some mechanical and hydrological properties of polymer-treated tailings.

2.3. Determination of Physical Properties

The specific gravity of the untreated (raw) and polymer-treated slurry samples after oven drying was determined using a helium pycnometer. Each measurement was repeated three times, and the average result was used to calculate porosity and other consolidation properties [48]. The gravimetric water content of each sample was quantified by dividing the mass of the water by the oven-dry mass of the sample (105 °C), in accordance with ASTM Standard D4959 [49]. To estimate the porosity and the void ratio of the materials, the dry density of the sample was calculated using the measured dried mass and volume of the sample (ASTM Standard D7263) [50,51]. The particle size distribution (PSD) was determined by wet sieving, which is a more reliable method compared to other techniques, particularly in the case of flocculated materials [52]. Wet sieving involved 10 stacked sieves, sized from 1000 μm to 38 μm, followed by a hydrometer analysis for particles under 38 μm. Testing adhered to AS 1289.3.6.1 [53] and AS 1289.3.6.3 standards [54].

2.4. Synchrotron-Sourced X-Ray Tomography

The internal structure of the polymer-treated sample was studied by X-Ray computer-tomography (CT) at Hutch 2B of the Imaging and Medical Beamline (IMBL) at the Australian Synchrotron. To capture high-resolution images, a custom-designed 'Ruby' detector was used, consisting of a terbium-doped gadolinium oxysulfide (Gadox, P43) scintillator (12 μm thickness) [55]. A PCO edge sensor equipped with a Nikon Micro-Nikkor 105 mm/f2.8 macro lens provided crisp images and precise measurements (the sensor was controlled using a motorised system and was protected from direct and scatter beam radiation by a mirror). During the experiment, the system was tuned to produce 2560×2560 pixel images, giving a field of view of 33.5 mm with a pixel size of 13.1 μm. The presentation of wet thickened polymer-treated material to the monochromatic X-Rays (30 keV) was not without challenges, and several configurations were explored to provide optimum 3D tomographic information. The thickened slurry was immobilised on glass slides with minimal disruption using a modified version of the doctor blading technique [56]. Each tomographic scan was collected over a 180° range in 0.20° steps, resulting in 900 views in total, with an exposure time of ~1.5 s per view.

2.5. Consolidation Test

Consolidation was completed as a drained test using a cylindrical slurry cell (volume 2655 cm^3 with a cross-sectional area of 177 cm^2), as shown in Figure 2. Constant initial rates of loading and step loading were used for both the flocculated and unflocculated samples. Loading rates of 0.1, 0.2, 0.4, 0.8, 1.6, and 3.2 kPa/min for loading steps of 20, 40, 80, 160, 320, and 500 kPa were applied to consolidate the samples. Each loading step was permitted to consolidate the materials for a maximum 24 h and the excess pore water pressure (PWP) was logged at the base of the sample. This gradual loading method best represented the continuous deposition of the tailing into a TSF and the above-mentioned approach for applying stress from the top in 24 h cycles was selected based on previous work, to mimic the continuous deposition of tailings in a TSF [13] and the results of preliminary testings. The drainage of water was allowed across the top surface to imitate field conditions. After each loading step, the allocated time was sufficient to consolidate the sample and to dissipate excess PWP [13].
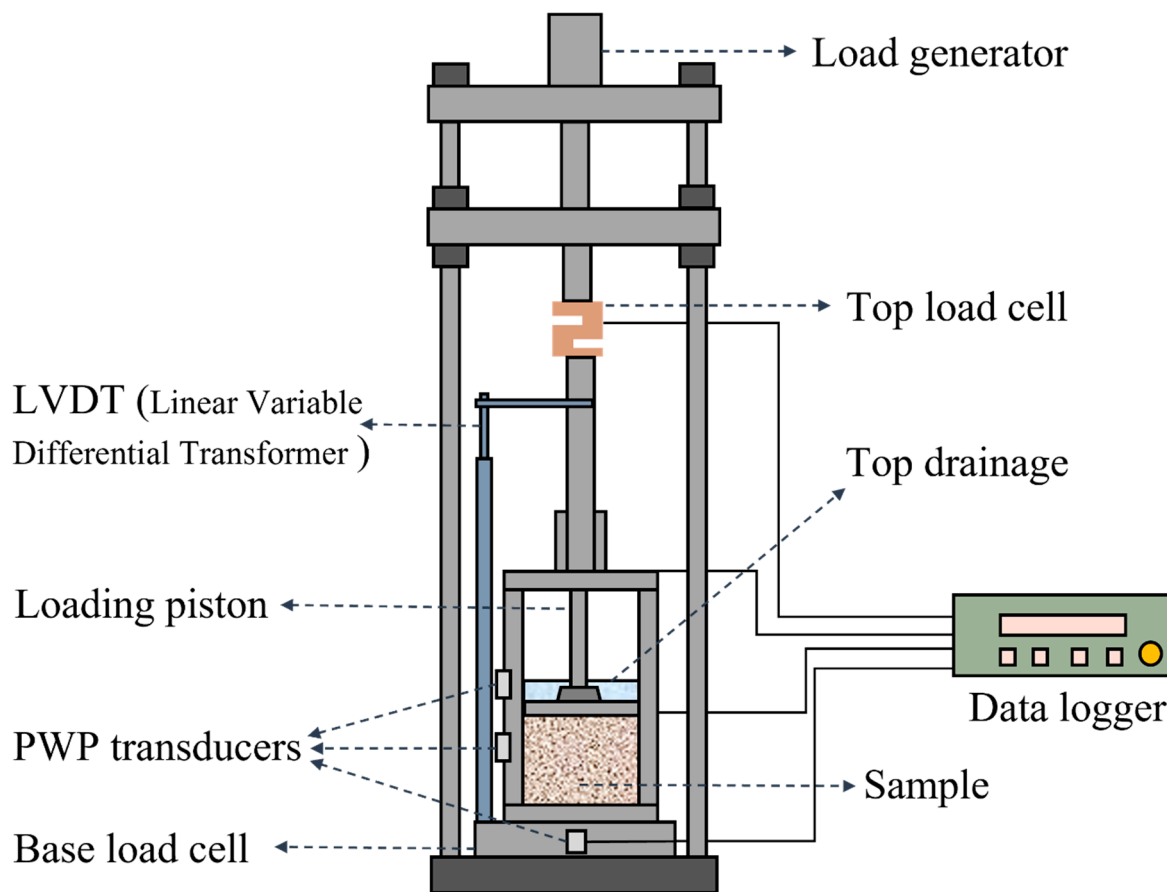
Figure 2. Schematic of slurry consolidometer.

2.6. Determination of Hydraulic Properties

To analyse the samples for their soil physical properties, water retention curves (WRC) were determined by initially desiccating each sample to a water potential of −1, −2, and −3 kPa for 24 h using a sand-based tension table. Both untreated and treated samples were placed in soil core holders (5.6 cm ID and 4 cm depth); however, due to the high-water content in untreated samples, settling was allowed for 48 h before transferring sediment to the core holders. A vacuum was applied to achieve a lower matric suction; the soil cores were placed on a porous plate for 4 days, 6 days, and 5 days sequentially to achieve water contents of −10, −30, and −50 kPa [57]. The last step was desiccation at −500 kPa using a pressure plate extractor (1500F1; Soil Moisture Equipment Corp., Santa Barbara, CA, USA) for 3 weeks. To determine the volumetric water content, the samples were weighed, and their shrinkage monitored and recorded after each desiccation step. After the final step, samples were dried at 105 °C for at least 24 h to calculate the bulk density. For the untreated and treated slurry, three representative samples were tested and the average results reported [58].

Several empirical models are available to predict the relationship between a specific, porous soil and its unsaturated soil properties such as shear strength and hydraulic conductivity through WRC data [59]. For the PAT and raw tailing materials in this study, uni-modal and bi-modal van Genuchten empirical models were applied, respectively, as the best fit of the experimental data [19]. To analyse the water content of the materials after gravitational drainage (water-holding capacity), the water potentials at field capacity were determined using the following equation [60]:

$$\psi_{FC} = \frac{1}{\alpha} \left(\frac{n-1}{n} \right)^{\frac{(1-2n)}{n}} \tag{1}$$

Then, the volumetric water contents were calculated after fitting the data to gain parameters based on the van Genuchten model [61] as follows:

$$\theta_{(\psi)} = \theta_r + \frac{\theta_s - \theta_r}{\left[1 + \left(\alpha|\psi|^n\right)\right]^{1-\frac{1}{n}}} \tag{2}$$

where $\theta(\Psi)$ is the water content (L^3/L^3); $|\Psi|$ is the suction pressure (L); θ_s and θ_r are the saturated and residual water content (L^3/L^3), respectively; α is the inverse of the air entry suction (1/L); and n is the measure of the pore size distribution [62]. It is suggested that for aggregated soils, a more flexible retention function should be used to provide a better fitting of experimental data [63]. Durner proposed a linear superposition of van Genuchten type sub-curves to yield the following expression for a multimodal retention as follows:

$$\theta_{(\psi)} = \sum_{i=1}^{k} w_i \left[1 + \left(\alpha_i|\psi|^{n_i}\right)\right]^{-m_i} \tag{3}$$

where the integer *k* indicates the modality of the model; and w_i are the weighting factors for the subcurves, subject to the constraints $0 < w_i < 1$ and summation of w_i is 1. In addition, α, n_i, and m_i ($m = 1 - 1/n$) are the curve-shape parameters of the subcurves, as in the unimodal case.

The saturated hydraulic conductivity of the soil samples was determined using a constant head permeability test [64]. The hydraulic conductivity test followed the method described by Reading et al. [65]. Deionized (DI) water was introduced to the columns from the bottom of the soil cores and the volume of water passing through the soil cores was determined to calculate the flow rate and then the hydraulic conductivity using Darcy's law [66].

3. Results and Discussions

3.1. Distribution of Applied Stress and Settling Behaviours

Figure 3 shows the extent of settlement in terms of the volume of the settled sediments (mL) and the recorded stress at the bottom of the samples (kPa) for both the untreated and PAT samples. Prior to starting the test, the friction between the piston (seal) and the cylinder wall was monitored to ensure that an appropriate stress was applied on top of the sample. Immediately after overcoming the friction by the applied load from the top, the stress was transferred into the base of the sample leading to consolidation. The friction loss between the specimen and cell wall was calculated using the following equation, in which the σ_t is the applied load at the top (kPa), and σ_b is the measured stress at the base (kPa):

$$Friction\ loss\ (\%) = \left(\frac{(\sigma_t - \sigma_b)}{\sigma_t}\right) \times 100 \tag{4}$$

Over the course of the test, approximately 68% of the applied stress was transferred to the base in the PAT sample, compared to 59% in the raw slurry. Higher friction losses in the raw slurry are likely due to its greater number of smaller particles, creating more contact points with the cell wall. This observation aligns with the reported friction loss ranges (10%–50%) for tailings slurries in similar studies [28]. This behaviour can also be related to the raw slurry conditions in the early stage of the test, during which negligible effective stress was generated [36,67].
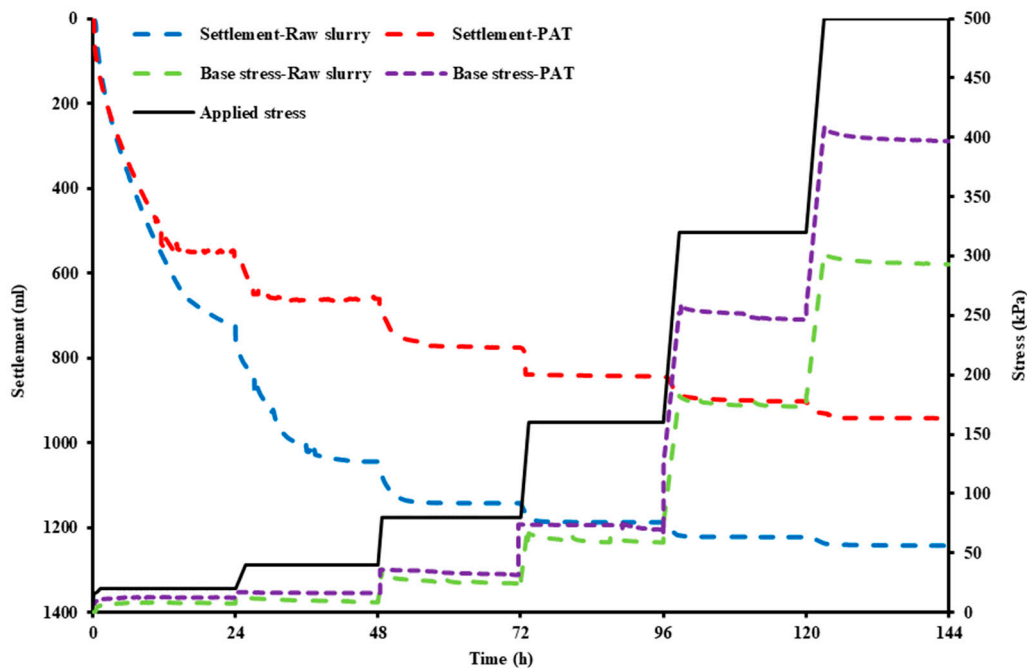
Figure 3. Applied stress, settlement, and base stress results for raw slurry and PAT samples over time.

The time required to reach a stable settlement varied significantly between samples. For instance, the raw slurry showed 60% greater settlement than the PAT sample within the first 48 h. The first loading cycle (20 kPa) took around 12 h for the PAT sample to reach the stable condition. Greater settlement of the raw slurry over the first two cycles led to a larger final settlement at the end of the test compared to the PAT sample, which had already lost most of its water content during the inline flocculation process. While the persistence of flocculated structures formed by acrylamide/acrylate copolymers can limit further settlement, the formation of such structures during inline flocculation could have potential benefits for tailings rehabilitation if the inter-aggregate pores are wide enough and persist to create higher pore conductivity and connectivity, thereby maintaining the convective flow of water and air [68].

Less stress being transferred to the base of the raw slurry compared to the PAT sample could also be attributed to the former's lower initial solids concentration and fewer particle interactions. Variations in the rate and extent of settlement could affect the pore water pressure (PWP) at the base of each sample, which is correlated to the friction pattern during the test. In this regard, Figure 4 presents the PWP results for both samples.

Figure 4 shows that when stress was applied after the first load, the bottom PWP started to develop immediately, indicating the piston had good contact with the sample and that the sample was entirely saturated [69]. A very small response was recorded for the PAT sample at the initial loading cycle, which is very low compared to the higher loads. Response for the PWP dissipation of the raw slurry was observed from the second loading cycle (40 kPa), and following the dissipation of PWP, only about 40% of the applied stress was transmitted to the base of the cell, indicating a high friction loss. As the PWP dissipated, effective stresses were generated, and hence, wall friction developed.
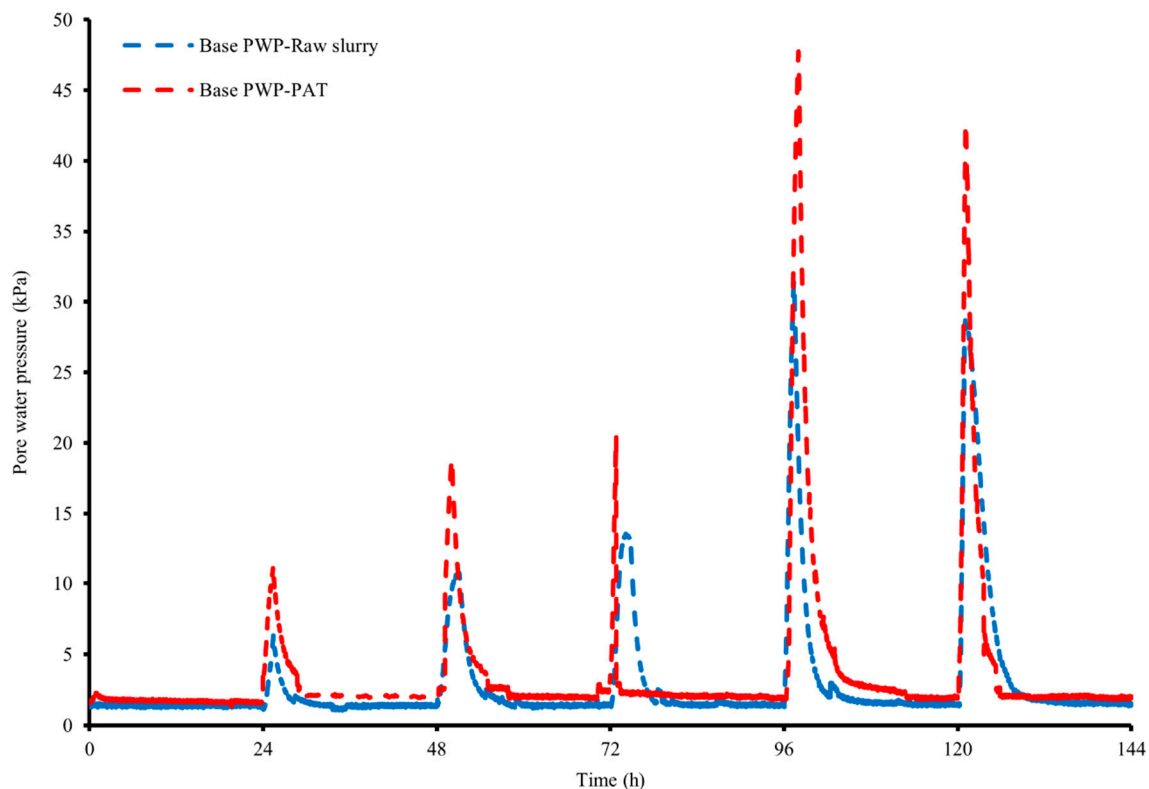
Figure 4. Pore water pressure results for raw slurry and PAT samples over time.

The results also showed PWP for the raw slurry and PAT samples rising in parallel with an initial increase with each applied stress cycle and thereafter a rapid dissipation, with the PAT sample giving a higher maximum pore pressure compared to the raw slurry. Thus, a combination of higher PWP and less contact points with the cell wall due to the presence of fewer but larger aggregates (Figure 5 presents PSD information for the samples) resulted in a greater base stress and consequently lower friction losses for the PAT sample. To understand the pattern of transferring applied stress to the base of the sample, there is a competition between the applied stress being mobilised along the cell wall in favour of the wall friction or interaction between particles [70]. The former leads to less stress at the bottom while the latter transfers more stress to the base, either in the form of PWP or base stress. This is in agreement with an earlier study in which numerical analysis was used to investigate the influence of the wall friction on large-strain consolidation tests under various loading sequences [71].

For the higher applied stresses (320 and 500 kPa), a greater proportion of the stress was transferred into the base. This was a consequence of reaching a higher solids concentration and the resulting lower void ratio transferring more stress to the water pore pressure. Additionally, the settlement behaviour of the materials shows an initial settlement of about 57% of the final settlement for the first loading cycle in both samples with no pore water pressure dissipated. On the other hand, a continuous sharp decreasing trend on settling was noted for the raw sample over the second 24 h period at 40 kPa, and this significant difference compared to the PAT settlement behaviour reflects the impact of changing the texture of the materials through polymer addition.
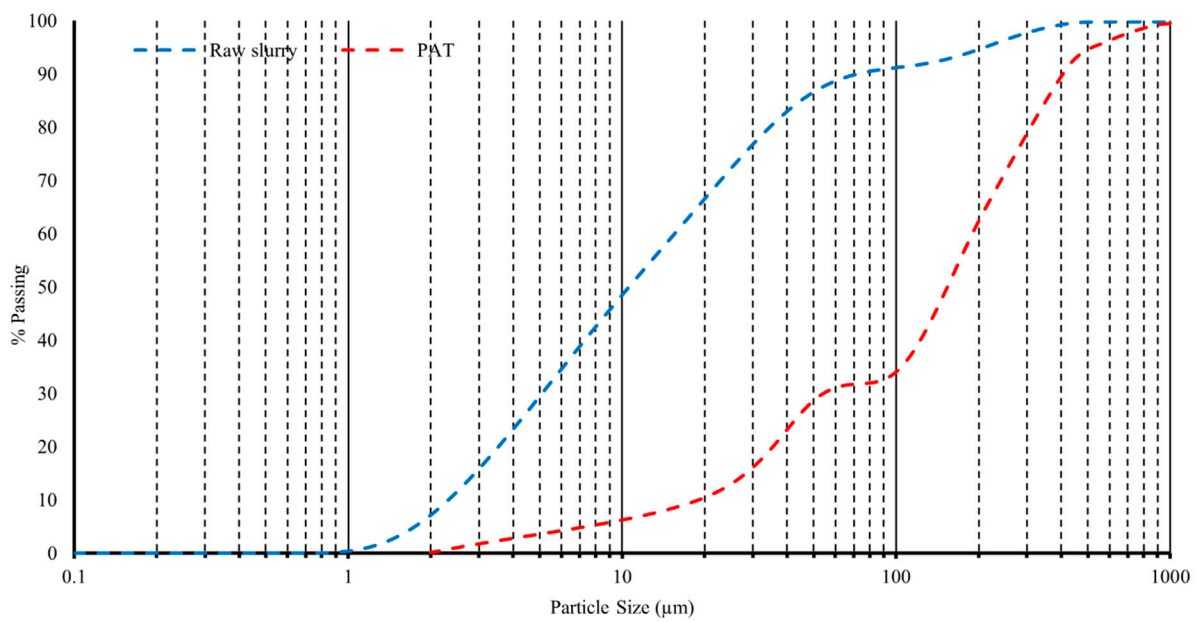
Figure 5. Particle size distribution of raw tailings and PAT samples by wet sieving.

3.2. Void Ratio and Dry Density Changes

The changes in void ratio for a standard kaolin-silt-sand slurry after inline flocculation with a conventional anionic polyacrylamide are presented in Figure 6 to better understand the impact of inline flocculation on the geotechnical and hydrological behaviour of tailings materials. The void ratio data of the PAT are higher than that of the raw slurry in all the applied loads. The initial moisture contents for the untreated tailings slurry and polymer amended sample before starting the test were 107% (with a void ratio of 2.6, and a dry density of 0.711 t/m^3) and 53% (with a void ratio of 1.6, and a dry density of 1.069 t/m^3), respectively. Similarly to previous studies [24,42,72] on the impacts of polymer treatment, the PAT materials resulted in different normal consolidation lines compared to the untreated tailings, which is mostly related to its water content. For several soils and tailings, initial slurry gravimetric water content has been shown to impact the final normal consolidation lines with lower slurry water content resulting in denser states [73,74].
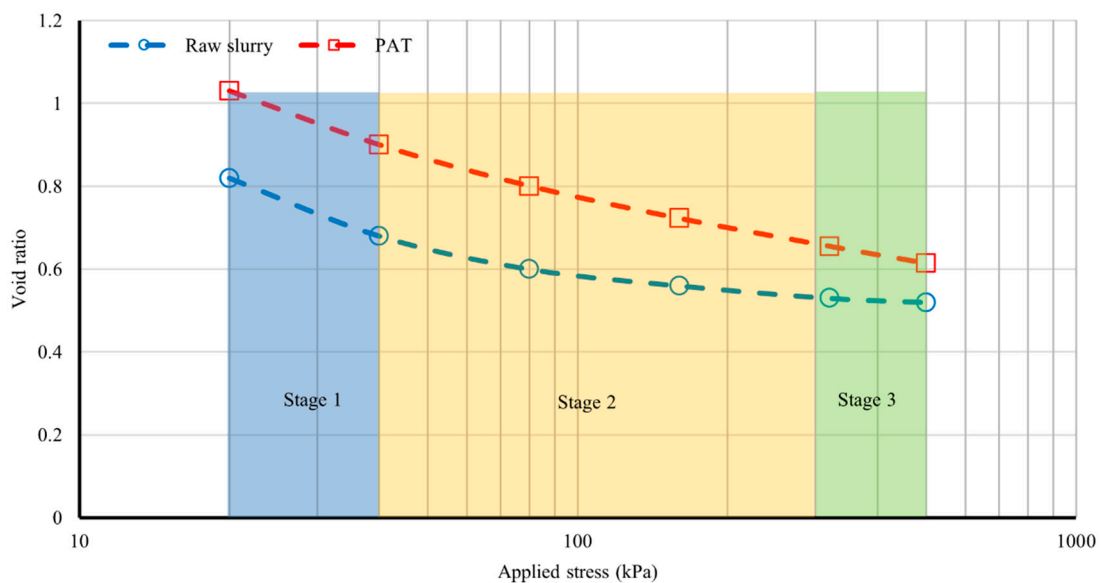

Figure 6. Void ratio over applied stress for raw and PAT samples.

Based on the recorded data, the initial void ratio of the raw slurry before applying any load was 2.6, while that of the polymer-treated sample was 1.6. Upon initial loading (20 kPa), the raw sample reached a void ratio of 0.81, while PAT maintained a higher void ratio (1.03) due to porous aggregate structures. This compression curve can be divided into three stages [75,76]. In the first stage, the void ratio decreases rapidly with the application of the initial applied stress. It can be inferred that the first stage of the compression was dominated by the suspension of larger particles and aggregates in a matrix of finer particles/aggregates, which are subject to initial compaction. In the second stage (40 to 300 kPa), or the transition stage, larger particles such as sand and silt compress, leading to compaction for both samples and a monotonic decline in the void ratio. Finally, in the last stage, the largest particles and aggregates made contact, and it is possible that fine particles moved into and filled the available voids, which led to a further slower decrease in void ratio before maximum compression was reached.

Based on soil mechanics theory, the slope of the graph can be used to calculate the overall compression index (C_c), the average consolidation coefficient (C_v), the coefficient of volume compressibility (M_v), and the saturated hydraulic conductivity (k). These parameters are summarised in Table 2 for the tailings sample before and after polymer treatment. C_v values were determined using the widely applied Casagrande logarithmic time-fitting method [13] and the equation below, in which H (in cm) is the average height of the sample before and after each loading step and t_{50} (in s) is the interpolated time required to reach 50% consolidation [33]:

$$C_v = \frac{0.197H^2}{t_{50}} \tag{5}$$

Table 2. Calculated average consolidation parameters and hydraulic conductivity.

Sample	C_c	C_v (cm²/s)	M_v (1/kPa)	K (m/s)
Raw slurry	1.05	0.0009	1.57×10^{-3}	3.24×10^{-10}
PAT	0.74	0.005	8.61×10^{-3}	1.99×10^{-7}

There are a number of relationships between the compression index (C_c) and other tailings properties such as void ratio, water content, and Atterberg limits for estimating and designing TSFs [77,78]. A larger value for the compression index signifies a greater compressibility. Consequently, a higher compressibility would result in a lower coefficient of consolidation C_v and more strain, which is necessary for developing the effective stress in the soil [79]. This interpretation is in broad agreement with the data presented in Table 2.

The void ratio variation with effective stress depends mainly on the solids concentration in the tailings sample. In this regard, the calculated data for the dry density of materials during each test under the applied stress is presented in Figure 7. Having different initial moisture contents for each sample resulted in substantial differences in the dry density, particularly throughout the lower applied stress. The greatest changes were observed for the raw slurry during the first two loading steps, increasing more than 0.6 t/m³ in dry density or 25% growth in solid mass percentage. Under these circumstances, a large quantity of water had to be released from the raw tailings under the applied pressure. In comparison, the changes in dry density were smaller for the PAT, as it had already been dewatered during inline flocculation treatment and therefore had a more stable condition under load.

After applying all loading stages, the final dry density of PAT reached 1.75 t/m³, which is more than that of the raw slurry (1.60 t/m³) and means that the amount of the water released during the polymer treatment under saline conditions was sufficient to improve the density. X-Ray tomography showed that the flocculated material produced at high solids and elevated dosages has a high degree of internal porosity, manifesting as discreet voids rather than an inter-connected pore structure (Figure 8). This raises the potential for the additional release of inter- and intra-aggregate water, particularly under

mild shear. In contrast, fine clay particles in the raw slurry struggle to release the contained water. The difference between the PAT and the raw slurry samples' dry density is reduced by increasing the applied stress.
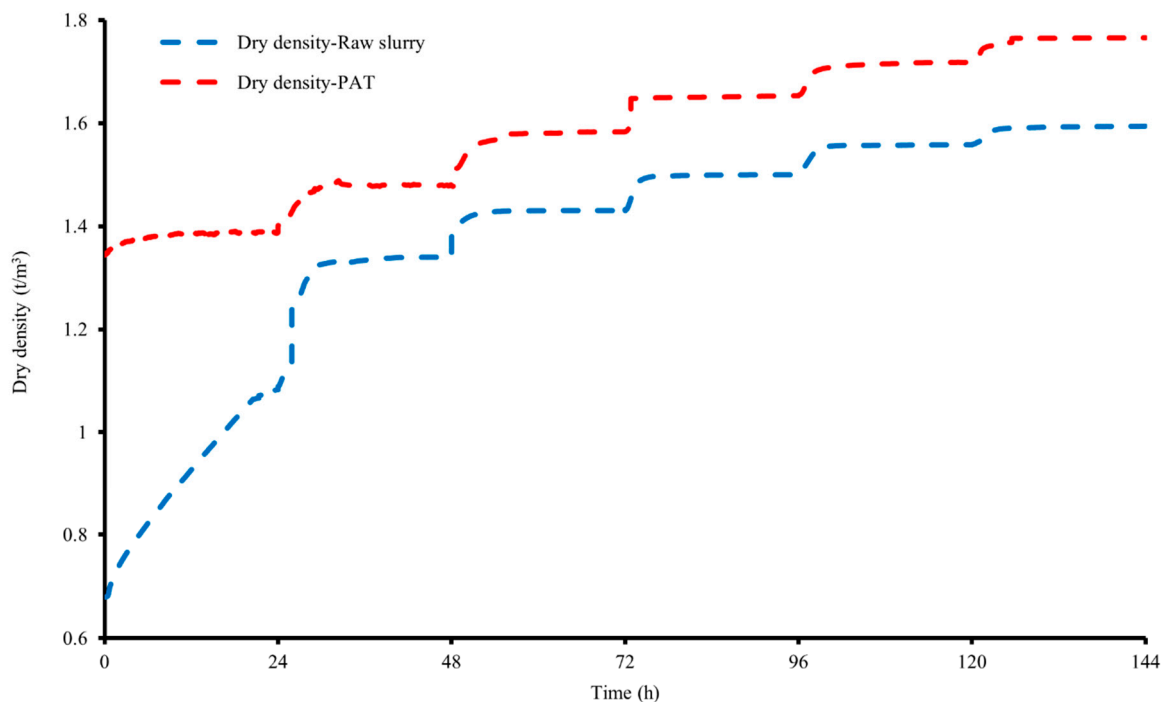

Figure 7. Comparison of dry density of untreated and PAT samples.

The raw unflocculated slurry did not have any rigidity or observable pores (not shown). Figure 8 shows a selected cross-sectional view of the PAT sample and 3D reconstructions of the internal pore space. Preliminary analysis indicates that PAT material produced at high solids and extreme polymer dosages has an abundance of micropores in the form of discrete voids with little inter-connectivity between them. Wells et al. [80] showed the importance of applying the correct shear regime for optimal water release from flocculated clay-rich oil sands tailings. The authors noted that some degree of aggregate breakage was needed to secure the largest water returns, with further over-shearing resulting in minimal water release. When considered in the context of the current X-Ray tomography results, it appears that the low-shear conditioning of the flocculated material can result in additional water being expelled from internal voids through the creation of new flow paths.

Among other factors (e.g., mineralogy), it is well known that the presence of fine particles in the tailings can lead to a higher compressibility [81–83]. In this study, it was found that inline polymer treatment can alter the properties of the deposited materials, resulting in significant effects on compressibility that may offer closure and rehabilitation benefits in some applications. In this context, the effect of polymer treatment on other parameters such as the hydraulic conductivity, the rate of consolidation, and the structure of the porous media is investigated in the next section.

The microstructural characteristics of PAT, particularly the presence of discrete micropores, play a pivotal role in influencing the material's macroscopic mechanical and hydrological properties. This distinct pore structure facilitates more efficient drainage under lower loads, as evidenced by PAT's higher hydraulic conductivity, and faster pore water pressure (PWP) dissipation rates compared to untreated tailings. The discrete voids created through polymer flocculation act as isolated reservoirs that, under mild shear, can release entrained water, enhancing overall water recovery from the material. This structural distinction contributes to PAT's lower compressibility and faster consolidation rate, which are advantageous in managing tailings' stability and long-term rehabilitation outcomes.
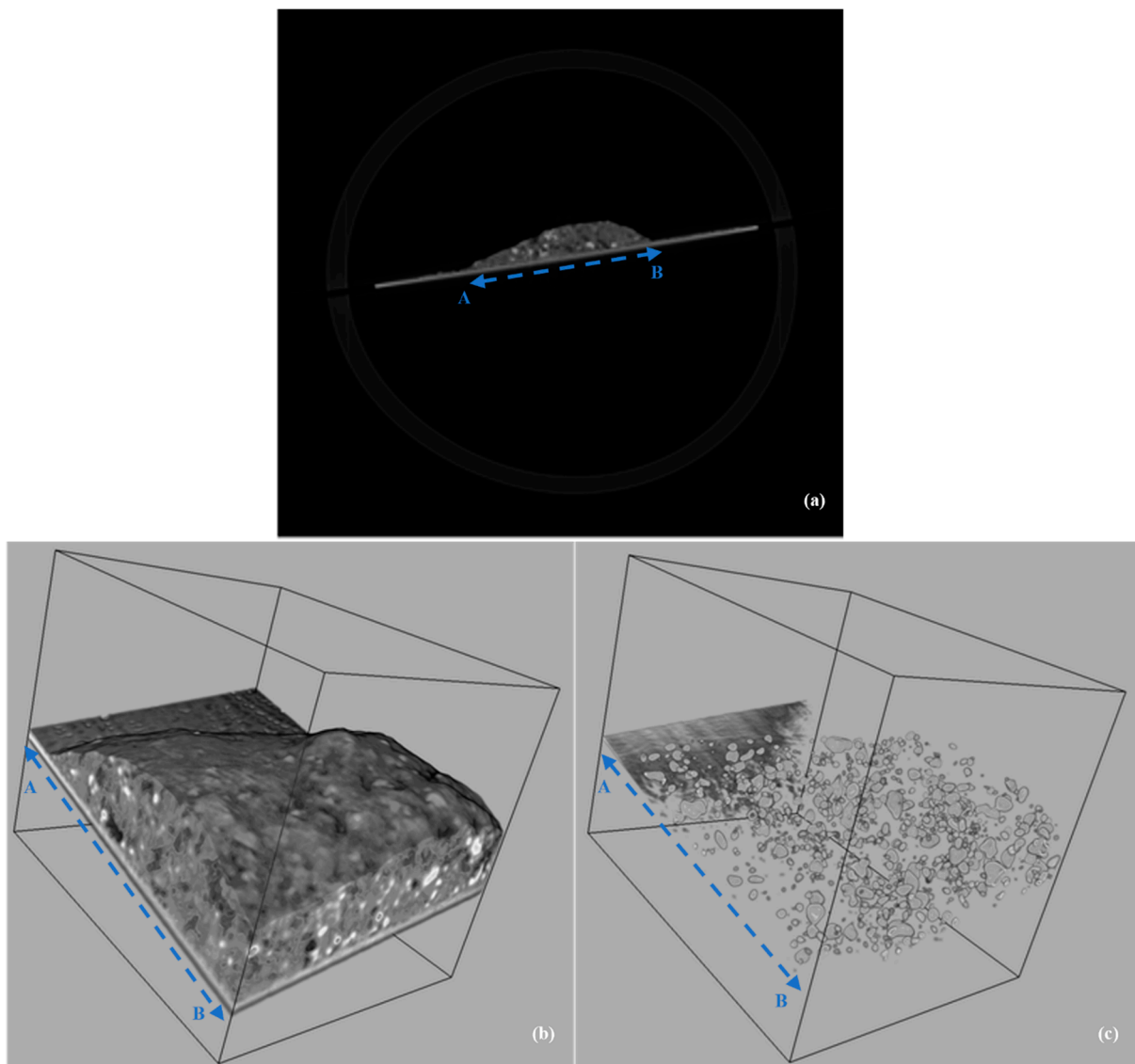
Figure 8. (**a**) X-Ray CT cross-sectional views of PAT sample, (**b**) presence of sand particles and voids in the material, and (**c**) internal porosity.

Comparative studies, such as those by Wells et al. [80] (on flocculated clay-rich oil sands tailings), underscore the benefits of a well-tuned shear regime in promoting water release from polymer-treated tailings. However, while previous research highlighted the need for moderate aggregate breakage, the present study demonstrates that PAT, with its discrete pore structure, can achieve significant water release without extensive breakage. This finding suggests that inline polymer treatment at high solids and elevated dosages may present a unique mechanism that enhances drainage and stability. The PAT's microstructure, with large, robust aggregates and isolated micropores, ensures faster water release and reduced consolidation time, supporting a more sustainable approach to tailings management, especially under high-solids and saline conditions.

3.3. Rate of Consolidation and Hydraulic Conductivity

The coefficient of consolidation (C_v) and hydraulic conductivity from bottom excess pore pressure dissipation are plotted as a function of applied stress in Figure 9. Hydraulic conductivity (k) can be calculated reliably from the consolidation test results by multiplying the C_v (m^2/s) by the volume rate of compressibility M_v (1/Pa) and the unit weight of water (kN/m^3) [84]. PAT materials exhibit a higher hydraulic conductivity and a more

rapid rate of consolidation across the range of the vertical stresses tested. To confirm the impact of the polymer treatment on the hydrological properties of the materials without applying stress on top, the constant head technique for measuring saturated hydraulic conductivity was carried out in duplicate for each sample and the results were 2.1×10^{-9} and 8.8×10^{-5} m/s for the raw tailings and PAT samples, correspondingly. These results are very close to the calculated saturated hydraulic conductivity under the initial loading condition before consolidating the material under pressure.
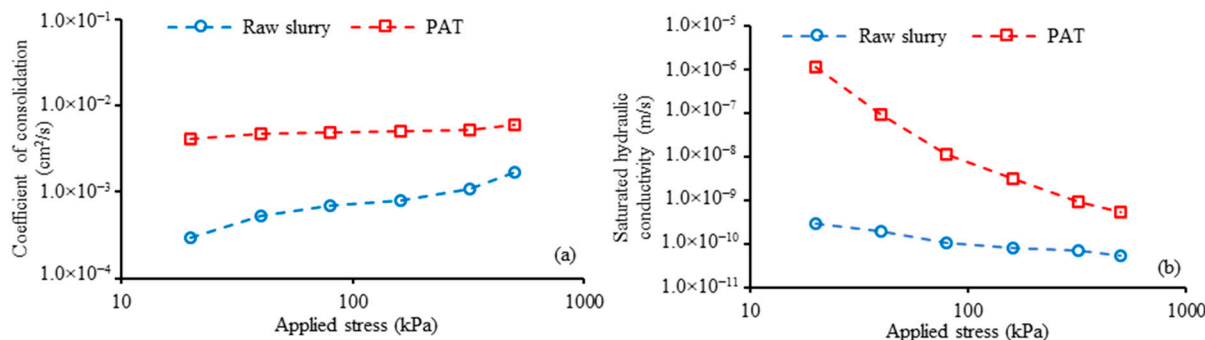

Figure 9. (**a**) Coefficient of consolidation (Cv) and (**b**) hydraulic conductivity (k) for both samples over applied stress.

The variation in the coefficient of consolidation with each incremental loading step was greater for the untreated sample, suggesting that it cannot easily lose the water around its structure and clay particles. This resulted in not only a lower rate of consolidation, but also produced material with a lower dry density and consequently poor saturated hydraulic conductivity. Saturated hydraulic conductivity data indicated that the polymer treatment resulted in changes to the materials allowing water to be expelled under lower loads. However, under higher stresses, both materials showed comparably small values of hydraulic conductivity that were indicative of a well-consolidated state [85]. Similar trends showing a greater hydraulic conductivity and higher rate of consolidation have been reported in other studies of polymer addition to different tailings, which indicate that polymer addition is inducing changes to the material's structure [81,86].

The significant difference between the particle size distribution of samples (Figure 5) clarifies the results obtained for hydraulic conductivity. While large aggregates are fragile and prone to breakage, their core structure is expected to be stronger in this application, and possibly a little larger when formed under high-dosage/high-solids conditions [46]. The PAT sample with larger aggregates and discrete void structure (shown in the X-Ray CT images in Figure 8) drains and dissipates PWP faster because of its higher hydraulic conductivity. After increasing the applied stress, variation in the hydraulic conductivity was greater for the PAT sample compared to the raw untreated tailings. The recorded hydraulic conductivity of PAT shows a reduction from 10^{-6} to 10^{-9} during the consolidation test; however, the minimum value at the highest applied stress is still higher than the maximum calculated hydraulic conductivity for the raw tailings sample. As discussed earlier, it appears that the pathways for releasing entrained water are blocked to some degree by fine particles and aggregates filling the voids and channels. This results in a reduction in hydraulic conductivity during the consolidation phase. That the primary consolidation for the raw untreated slurry took more than double the time of the PAT sample is consistent with a lower permeability and longer length of the drainage path. As hydraulic conductivity strongly impacts the time required for consolidation, it is one of the most important parameters in designing TSFs and predicting the stability of tailings [85].

3.4. Water Retention Curve (WRC) Anaysis

WRCs provide quantification around the ease of water removal from porous media by changing the water content through controlled suction [87]. WRCs were employed to

evaluate the air entry values (AEVs) for each sample and to characterise their properties across a range of suctions by changing the soil wetness, as illustrated in Figure 10. The amount of water remaining in the materials at equilibrium is a function of the sizes of the water-filled pores, so it is a function of the matric suction. This function can be quantified experimentally, and it is represented graphically by a curve known as the WRC [48].
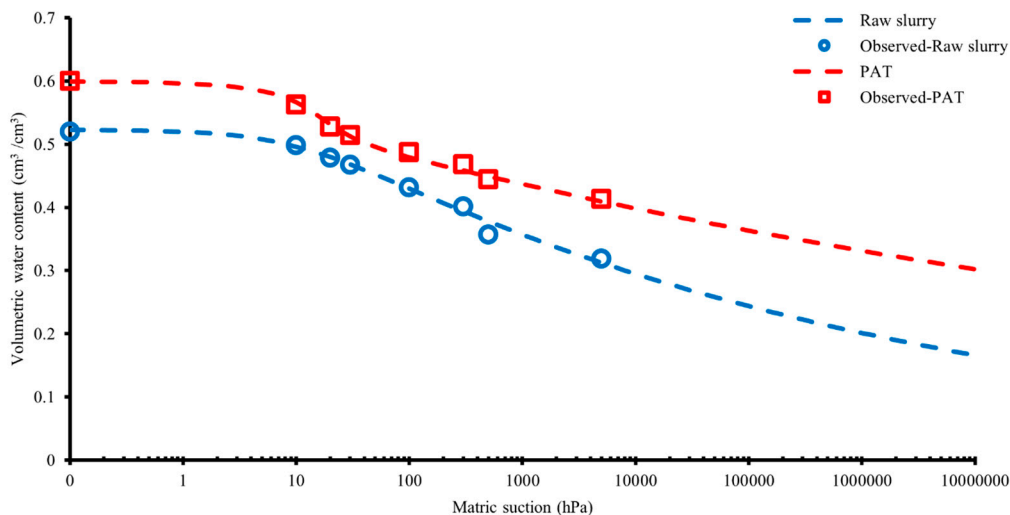

Figure 10. Comparison of the water retention curves for raw and PAT samples.

All calculations and parameters after fitting the data to the van Genuchten model (Equation (3)) are reported in Table 3. The macropore volume and the mesopore volume calculated for each sample show the difference in pore structure after polymer treatment.

Table 3. Water retention characteristics of both raw slurry and PAT samples.

Sample	α_1 (kPa^{-1})	α_2 (kPa^{-1})	n_1	n_2	w	θs	θ_r	θ_{FC}	θ_{WP}	Macropore Volume (cm^3/cm^3)	Mesopore Volume (cm^3/cm^3)
Raw Slurry	0.099	-	1.083	-	-	0.52	0	0.43	0.28	0.09	0.15
PAT	0.07	0.2	3	1.04	0.1	0.6	0	0.48	0.39	0.12	0.09

α: inverse of the air entry suction; n: measure of the pore size distribution; w: weighting factor for bi-modal WRC; FC: field capacity; WP: wilting point; s: saturated; r: residual.

At the start of each test, the materials were in equilibrium with free water at atmospheric pressure and the suction set to zero. Upon applying a small suction, no outflow was observed until a critical applied suction was reached, in which the larger pores released their entrapped water. The point at which water is displaced by air from the larger pores is called the air entry suction, which was only ~2 hPa for PAT and 8 hPa for the raw tailings, respectively. This value is generally small for well-aggregated and coarse samples compared to more fine-textured materials [48]. Increasing the matric suction results in the progressive removal of water from smaller pores. Only narrow, constrained pore geometries would be expected to retain any water under the very high matric suction of 5000 hPa.

The polymer-treated sample drained almost 50% more free water compared to the untreated slurry at field capacity (−100 hPa water potential) but can also retain more water within its aggregated mass. This material has higher infiltration rates in comparison with the raw slurry which contains finer particles. Practically, the polymer addition transforms some microporous media to the macropores structure in which the drainage expanded, and more water was readily conducted through the aggregates [88].

Water retention characteristic curves were presented to better understand the physical and soil-like properties of the created aggregates resulting from polymer addition and to

quantify the capacity of the material for holding and losing water through its porous texture. The addition of polymer to dewater the raw slurry altered the physical characteristics of the materials by changing the volumetric water content while increasing matric suction. These changes include (i) creating larger macropore volumes to drain more water easily, (ii) changing the field capacity and permanent wilting points of the raw tailing in favour of having a greater holding capacity, and (iii) improving the residual water content to prevent the strong wilting of the materials which cause the preferential flow. These modifications, plus the larger particle sizes, are linked with hydraulic conductivity and provide the conditions to move water through the structure of the tailings in favour of potential rehabilitation purposes for the long-term processes.

4. Conclusions

This study quantified the geotechnical and hydro-mechanical properties of untreated and polymer-amended tailings after inline flocculation under high-solids, dosage, and salinity conditions. The findings reveal that polymer treatment using an anionic poly-acrylamide significantly enhances tailings stability post-deposition. The key results are as follows:

- Polymer treatment increased the average rate of consolidation from 0.0009 to 0.005 cm^2/s and enhanced hydraulic conductivity from 3.24×10^{-10} to 1.99×10^{-7} m/s, supporting faster water drainage and more effective consolidation under lower loads.
- PAT samples displayed a higher void ratio, permeability, and hydraulic conductivity, leading to a ~50% increase in free water drainage at field capacity compared to the raw slurry. The air entry suction also decreased from 8 to 2 hPa, indicative of improved aggregate formation and a non-homogeneous structure even under saline conditions.
- Synchrotron X-Ray tomography confirmed that PAT has discrete, non-interconnected micropores, which could facilitate additional water release through new flow paths under mild shear.

These findings highlight the potential of polymer treatment to improve tailings stability and support sustainable tailings management, particularly in high-solids, saline environments. It should be noted, however, that these results were obtained for a single flocculant dosage, and the observed effects are therefore specific to this dosage. Future studies are recommended to explore the impact of varying flocculant doses on these parameters to fully understand the dose-dependent behaviour of polymer treatments in tailings stabilisation.

While this study provides valuable insights into the short-term mechanical and hydraulic behaviour of polymer-amended tailings, further research is needed to assess the long-term stability of these treated materials. Understanding the evolution of polymer-treated tailings over time, including factors like potential changes in microstructure, consolidation behaviour, and hydraulic conductivity, will be essential for developing sustainable tailings storage and rehabilitation strategies.

Conflicts of Interest: The authors declare no conflict of interest.

References

1. Arjmand, R.; Massinaei, M.; Behnamfard, A. Improving flocculation and dewatering performance of iron tailings thickeners. *J. Water Process Eng.* **2019**, *31*, 100873. [CrossRef]
2. Grabsch, A.F.; Fawell, P.D.; Adkins, S.J.; Beveridge, A. The impact of achieving a higher aggregate density on polymer-bridging flocculation. *Int. J. Miner. Process.* **2013**, *124*, 83–94. [CrossRef]
3. Liu, D.; Edraki, M.; Berry, L. Investigating the settling behaviour of saline tailing suspensions using kaolinite, bentonite, and illite clay minerals. *Powder Technol.* **2018**, *326*, 228–236. [CrossRef]
4. Dwari, R.K.; Mishra, B.K. Evaluation of flocculation characteristics of kaolinite dispersion system using guar gum: A green flocculant. *Int. J. Min. Sci. Technol.* **2019**, *29*, 745–755. [CrossRef]
5. Qi, C.; Ly, H.-B.; Chen, Q.; Le, T.-T.; Le, V.M.; Pham, B.T. Flocculation-dewatering prediction of fine mineral tailings using a hybrid machine learning approach. *Chemosphere* **2020**, *244*, 125450. [CrossRef]
6. Anstey, D.; Guang, R. Relationship between In-line polymer dose and tailings index. In Proceedings of the Tailings and Mine Waste Conference, Banff, Alberta, 7–10 November 2017; pp. 1–10.
7. Fawell, P.; Adkins, S.; Costine, A. Chapter 6: Reagents. In *Paste and Thickened Tailings—A Guide*; Australian Centre for Geomechanics: Perth, Australia, 2015; pp. 87–108.
8. Poncet, F. Method for Treating Mineral Sludge Above Ground Using Polymers. CA Patent 02682542, 23 October 2008.
9. McColl, P.; Scammell, S. Treatment of Mineral Material, Especially Waste Mineral Slurries Transferring Material with Dispersed Particulatesolids Asfluid to Deposition Area by Combining with Material Aqueous Solution of Water-Soluble Polymer. U.S. Patent 7901583B2, 2004.
10. Gaillard, N.; Poncet, F. Treating Sludge from Mining or Mineral Industry Before Spreading out into Soil, Comprises Contacting the Sludge with a Branched flocculant Such as a Water Soluble Organic Polymer Having a Specified Anionicity for a Specified Duration. U.S. Patent 2010/0105976 A1, 30 August 2010.
11. Costine, A.; Benn, F.; Fawell, P.; Edraki, M.; Baumgartl, T.; Bellwood, J. Understanding factors affecting the stability of inline polymer-amended tailings. In Proceedings of the 21st International Seminar on Paste and Thickened Tailings, Perth, Australia, 11–12 April 2018; pp. 103–116.
12. Avadiar, L.; Leong, Y.K.; Fourie, A. Effects of polyethylenimine dosages and molecular weights on flocculation, rheology and consolidation behaviors of kaolin slurries. *Powder Technol.* **2014**, *254*, 364–372. [CrossRef]
13. Islam, S.; Williams, D.J.; Llano-Serna, M.; Zhang, C. Settling, consolidation and shear strength behaviour of coal tailings slurry. *Int. J. Min. Sci. Technol.* **2020**, *30*, 849–857. [CrossRef]
14. O'Kelly, B.C. Undrained shear strength-water content relationship for sewage sludge. *Proc. Inst. Civ. Eng. Geotech. Eng.* **2013**, *166*, 576–588. [CrossRef]
15. Riley, T.; Reid, D.; Utting, L. Polymer-modified tailings deposition—Ongoing testing and potential storage efficiency opportunities. In Proceedings of the Paste 2015: Proceedings of the 18th International Seminar on Paste and Thickened Tailings, Cairns, Australia, 5–7 May 2015; pp. 139–152. [CrossRef]
16. Zhu, L.; Lyu, W.; Yang, P.; Wang, Z. Effect of ultrasound on the flocculation-sedimentation and thickening of unclassified tailings. *Ultrason. Sonochem.* **2020**, *66*, 104984. [CrossRef] [PubMed]
17. Liu, D.; Edraki, M.; Fawell, P.; Berry, L. Improved water recovery: A review of clay-rich tailings and saline water interactions. *Powder Technol.* **2020**, *364*, 604–621. [CrossRef]
18. Guang, R.; Longo, S. Application of in-line polymer addition for tailings disposal-learning and challenges part II. In Proceedings of the 20th International Seminar on Paste and Thickened Tailings, Beijing, China, 18 June 2017; pp. 371–379.
19. Ghirian, A.; Fall, M. Coupled thermo-hydro-mechanical-chemical behaviour of cemented paste backfill in column experiments. Part I: Physical, hydraulic and thermal processes and characteristics. *Eng. Geol.* **2013**, *164*, 195–207. [CrossRef]
20. Rankine, R.M.A. The Geotechnical Characterisation and Stability Analysis of BHP Billiton's Cannington Mine Paste Fill. Ph.D. Thesis, James Cook University, Townsville, Australia, 2004.
21. Komljenovic, D.; Stojanovic, L.; Malbasic, V.; Lukic, A. A resilience-based approach in managing the closure and abandonment of large mine tailing ponds. *Int. J. Min. Sci. Technol.* **2020**, *30*, 737–746. [CrossRef]
22. Watson, P.; Farinato, R.; Fenderson, T.; Hurd, M.; Macy, P.; Mahmoudkhani, A. Novel polymeric additives to improve oil sands tailings consolidation. In Proceedings of the Proceedings—SPE International Symposium on Oilfield Chemistry, The Woodlands, TX, USA, 11–13 April 2011; Volume 2, pp. 703–709.
23. Edraki, M.; Baumgartl, T.; Manlapig, E.; Bradshaw, D.; Franks, D.M.; Moran, C.J. Designing mine tailings for better environmental, social and economic outcomes: A review of alternative approaches. *J. Clean. Prod.* **2014**, *84*, 411–420. [CrossRef]
24. Jeeravipoolvarn, S.; Scott, J.D.; Chalaturnyk, R.J.; Shaw, W.; Wang, N. Sedimentation and consolidation of in-line thickened fine tailings. In Proceedings of the International Oil Sands Tailings Conference, Edmonton, AB, Canada, 7–10 December 2008; pp. 1–14.
25. Rodríguez, R.; Sánchez, M.; Ledesma, A.; Lloret, A. Experimental and numerical analysis of desiccation of a mining waste. *Can. Geotech. J.* **2007**, *44*, 644–658. [CrossRef]

26. Gibson, R.E.; England, G.L.; Hussey, M.J.L. The theory of one-dimensional consolidation of saturated clays. *Geotechnique* **1967**, *17*, 261–273. [CrossRef]

27. Qin, J.; Zheng, J.; Li, L. An analytical solution to estimate the settlement of tailings or backfill slurry by considering the sedimentation and consolidation. *Int. J. Min. Sci. Technol.* **2021**, *31*, 463–471. [CrossRef]

28. Shokouhi, A.; Zhang, C.; Williams, D.J. Settling, consolidation and desiccation behaviour of coal tailings slurry. *Min. Technol. Trans. Inst. Min. Metall.* **2018**, *127*, 1–11. [CrossRef]

29. Shokouhi, A.; Williams, D.J. Volume change behaviour of mixtures of coarse coal reject and tailings. *Trans. Institutions Min. Metall. Sect. A Min. Technol.* **2017**, *126*, 163–176. [CrossRef]

30. Indraratna, B. Geotechnical characterization of blended coal tailings for construction and rehabilitation work. *Q. J. Eng. Geol.* **1994**, *27*, 353–361. [CrossRef]

31. Rujikiatkamjorn, C.; Indraratna, B.; Chiaro, G. Compaction of coal wash to optimise its utilisation as water-front reclamation fill. *Geomech. Geoengin.* **2013**, *8*, 36–45. [CrossRef]

32. Li, R.; Zhou, G.; Mo, P.-Q.; Hall, M.R.; Chen, J.; Chen, D.; Cai, S. Behaviour of granular matter under gravity-induced stress gradient: A two-dimensional numerical investigation. *Int. J. Min. Sci. Technol.* **2021**, *31*, 439–450. [CrossRef]

33. Shukla, S.K.; Sivakugan, N.; Das, B.M. Methods for determination of the coefficient of consolidation and field observations of time rate of settlement—An overview. *Int. J. Geotech. Eng.* **2009**, *3*, 89–108. [CrossRef]

34. Bo, M.W.; Choa, V.; Wong, K.S. Compression tests on a slurry using a small-scale consolidometer. *Can. Geotech. J.* **2002**, *39*, 388–398. [CrossRef]

35. Li, R.; Zhou, G.; Yan, K.; Chen, J.; Chen, D.; Cai, S.; Mo, P.Q. Preparation and characterization of a specialized lunar regolith simulant for use in lunar low gravity simulation. *Int. J. Min. Sci. Technol.* **2021**, *32*, 1–15. [CrossRef]

36. Bo, M.W.; Wong, K.S.; Choa, V. Constant rate of displacement test on ultra-soft soil. *Proc. Inst. Civ. Eng.-Geotech. Eng.* **2008**, *161*, 129–135. [CrossRef]

37. Islam, S.; Shang, J.Q. Coagulation enhanced electrokinetic settling of mature fine oil sands tailings. *Int. J. Min. Sci. Technol.* **2019**, *29*, 199–208. [CrossRef]

38. Boshrouyeh Ghandashtani, M.; Costine, A.; Edraki, M.; Baumgartl, T. The impacts of high salinity and polymer properties on dewatering and structural characteristics of flocculated high-solids tailings. *J. Clean. Prod.* **2022**, *342*, 130726. [CrossRef]

39. Boshrouyeh Ghandashtani, M.; Edraki, M.; Baumgartl, T.; Costine, A.; Amari, S. Investigation of the Attenuation and Release of Cu^{2+} Ions by Polymer-Treated Tailings. *Minerals* **2022**, *12*, 846. [CrossRef]

40. Lee, B.J.; Schlautman, M.A. Effects of Polymer Molecular Weight on Adsorption and Flocculation in Aqueous Kaolinite Suspensions Dosed with Nonionic Polyacrylamides. *Water* **2015**, *7*, 5896–5909. [CrossRef]

41. Jeldres, R.; Yang, T.; Costine, A.; Fawell, P.; Bellwood, J. The impact of high salinity and seawater on aggregate structures in clay tailings flocculation. In Proceedings of the Paste 2020: 23rd International Conference on Paste, Thickened and Filtered Tailings, Santiago, Chile, 2–6 November 2020; Quelopana, H., Ed.; Gecamin Publications PP: Santiago, Chile, 2020; pp. 1–8.

42. Reid, D.; Fourie, A. Laboratory assessment of the effects of polymer treatment on geotechnical properties of low-plasticity soil slurry. *Can. Geotech. J.* **2016**, *53*, 1718–1730. [CrossRef]

43. Bray, J.D. and R.B.S. Assessment of the Liquefaction Susceptibility of Fine-Grained Soils. *J. Geotech. Geoenvironmental Eng.* **2006**, *132*, 1165–1177. [CrossRef]

44. Seed, R.B.; Cetin, K.O.; Moss, R.E.; Kammerer, A.M.; Wu, J.; Pestana, J.M.; Riemer, M.F.; Sancio, R.B.; Bray, J.D.; Kayen, R.E.; et al. Recent Advances in Soil Liquefaction Engineering: A Unified and Consistent Framework. In Proceedings of the 26th Annual ASCE Los Angeles Geotechnical Spring Seminar, Long Beach, CA, USA, 30 April 2003.

45. Owen, A.T.; Fawell, P.D.; Swift, J.D.; Farrow, J.B. The impact of polyacrylamide flocculant solution age on flocculation performance. *Int. J. Miner. Process.* **2002**, *67*, 123–144. [CrossRef]

46. Costine, A.; Fawell, P.; Chryss, A.; Dahl, S.; Bellwood, J. Development of test procedures based on chaotic advection for assessing polymer performance in high-solids tailings applications. *Processes* **2020**, *8*, 1–20. [CrossRef]

47. Fawell, P.D.; Costine, A.D.; Grabsch, A.F. Why small-scale testing of reagents goes wrong. In Proceedings of the Paste 2015: 18th International Seminar on Paste and Thickened Tailings, Cairns, Australia, 5–7 May 2015; Jewell, R., Jewell, R., Fourie, A.B., Fourie, A.B., Eds.; Australian Centre for Geomechanics PP: Crawley, Australia, 2015; pp. 153–165.

48. Hillel, D. *Introduction to Soil Physics*; Academic Press: New York, NY, USA, 1982; ISBN 0123485207.

49. *ASTM D4959*; Standard Test Method for Determination of Water (Moisture) Content of Soil by Direct Heating. ASTM International: West Conshohocken, PA, USA, 2021. [CrossRef]

50. Roshani, A.; Fall, M.; Kennedy, K. A column study of the hydro-mechanical behavior of mature fine tailings under atmospheric drying. *Int. J. Min. Sci. Technol.* **2017**, *27*, 203–209. [CrossRef]

51. *ASTM D7263*; Standard Test Methods for Laboratory Determination of Density (Unit Weight) of Soil Specimens. ASTM International: West Conshohocken, PA, USA, 2021. [CrossRef]

52. Wu, S.; Zhu, W.; Min, F.; Fan, X. A Test Method for Measuring Floc Size of Slurry. *Geotech. Test. J.* **2018**, *41*, 20170168. [CrossRef]

53. *AS 1289.3.6.1*; Methods of Testing Soils for Engineering Purposes: Soil Strength and Consolidation Tests—Determination of the Particle Size Distribution of a Soil—Standard Method of Analysis by Dry Sieving. Standards Australia: Sydney, Australia, 2009.

54. *AS 1289.3.6.3*; Methods of Testing Soils for Engineering Purposes: Soil Strength and Consolidation Tests—Determination of the Particle Size Distribution of a Soil—Standard Method of Analysis by Wet Sieving. Standards Australia: Sydney, Australia, 2009.

55. Scarlett, N.V.Y.; Tyson, P.; Fraser, D.; Mayo, S.; Maksimenko, A. Synchrotron X-Ray CT characterization of titanium parts fabricated by additive manufacturing. Part II. Defects. *J. Synchrotron Radiat.* **2016**, *23*, 1015–1023. [CrossRef]

56. Yang, H.; Jiang, P. Large-scale colloidal self-assembly by doctor blade coating. *Langmuir* **2010**, *26*, 13173–13182. [CrossRef]

57. Shaygan, M.; Reading, L.P.; Baumgartl, T. Effect of physical amendments on salt leaching characteristics for reclamation. *Geoderma* **2017**, *292*, 96–110. [CrossRef]

58. Kim, K.Y.; Chae, K.J.; Choi, M.J.; Yang, E.T.; Hwang, M.H.; Kim, I.S. High-quality effluent and electricity production from non-CEM based flow-through type microbial fuel cell. *Chem. Eng. J.* **2013**, *218*, 19–23. [CrossRef]

59. Fredlund, D.G.; Rahardjo, H. *Soil Mechanics for Unsaturated Soils*; John Wiley & Sons, Inc: New York, NY, USA, 1993.

60. de Oliveira, R.A.; Ramos, M.M.; de Aquino, L.A. *Irrigation Management*; Elsevier Inc.: Amsterdam, The Netherlands, 2015; ISBN 9780128022399.

61. Assouline, S.; Or, D. The concept of field capacity revisited: Defining intrinsic static and dynamic criteria for soil internal drainage dynamics. *Water Resour. Res. Res.* **2014**, *50*, 4787–4802. [CrossRef]

62. Hilton, M.; Shaygan, M.; McIntyre, N.; Baumgartl, T.; Edraki, M. The effect of weathering on salt release from coal mine spoils. *Minerals* **2019**, *9*, 760. [CrossRef]

63. Zurmühl, T.; Durner, W. Determination of Parameters for Bimodal Hydraulic Functions by Inverse Modeling. *Soil Sci. Soc. Am. J.* **1998**, *62*, 874–880. [CrossRef]

64. Klute, A.; Dirksen, C. Hydraulic conductivity and diffusivity: Laboratory methods. *Methods Soil Anal. Part 1 Phys. Mineral. Methods* **2018**, *9*, 687–734. [CrossRef]

65. Reading, L.P.; Baumgartl, T.; Bristow, K.L.; Lockington, D.A. Hydraulic conductivity increases in a sodic clay soil in response to gypsum applications: Impacts of bulk density and cation exchange. *Soil Sci.* **2012**, *177*, 165–171. [CrossRef]

66. Marshall, T.J.; Holmes, J.W.; Rose, C.W. *Soil Physics*, 3rd ed.; Cambridge University Press: Cambridge, UK, 1996; ISBN 9780521451512.

67. Monte, J.L.; Krizek, R.J. One-dimensional mathematical model for large-strain consolidation. *Géotechnique* **1976**, *26*, 495–510. [CrossRef]

68. Horn, R.; Smucker, A. Structure formation and its consequences for gas and water transport in unsaturated arable and forest soils. *Soil Tillage Res.* **2005**, *82*, 5–14. [CrossRef]

69. Bo, M.W.; Sin, W.K.; Choa, V.; Ing, T.C. Compression tests of ultra-soft soil using an hydraulic consolidation cell. *Geotech. Test. J.* **2003**, *26*, 310–319. [CrossRef]

70. Bo, M.W.; Choa, V.; Wong, K.S. Constant rate of loading test on ultra-soft soil. *Geotech. Test. J.* **2010**, *33*, 192–200. [CrossRef]

71. He, W.; Williams, D.; Shokouhi, A. Numerical study of slurry consolidometer tests taking into account the influence of wall friction. *Comput. Geotech.* **2017**, *91*, 39–47. [CrossRef]

72. Yao, Y.; Van Tol, F.; Van Paassen, L. The effect of Flocculant on the Geotechnical Properties of Mature Fine Tailimgs: An Experimental study. In Proceedings of the 3rd International Oil Sands Conference, Edmonton, AB, Canada, 3–5 December 2012; pp. 391–398.

73. Al-Tarhouni, M.; Simms, P.; Sivathayalan, S. Cyclic behaviour of reconstituted and desiccated–rewet thickened gold tailings in simple shear. *Can. Geotech. J.* **2011**, *48*, 1044–1060. [CrossRef]

74. Nocilla, A.; Coop, M.R.; Colleselli, F. The mechanics of an Italian silt: An example of 'transitional' behaviour. *Géotechnique* **2006**, *56*, 261–271. [CrossRef]

75. Wong, R.C.; Mills, B.N.; Liu, Y.B. Mechanistic Model for One-Dimensional Consolidation Behavior of Nonsegregating Oil Sands Tailings. *J. Geotech. Geoenvironmental Eng.* **2008**, *134*, 195–202. [CrossRef]

76. Zhang, X.; Lu, Y.; Yao, J.; Wu, Y.; Tran, Q.C.; Vu, Q.V. Insight into conditioning landfill sludge with ferric chloride and a Fenton reagent: Effects on the consolidation properties and advanced dewatering. *Chemosphere* **2020**, *252*, 126528. [CrossRef]

77. Akayuli, C.F.A.; Ofosu, B. Empirical Model for Estimating Compression Index from Physical Properties of Weathered Birimian Phyllites. *Electron. J. Geotech. Eng.* **2014**, *18*, 6135–6144.

78. Widodo, S.; Ibrahim, A.; Strasse, G.Z.; Sn, F.; Freiberg-germany, T.U.B.; University-sudan, A.N.; Clay, S. Estimation of Primary Compression Index (Cc) Using Physical Properties of Pontianak Soft Clay. *Int. J. Eng. Res. Appl.* **2012**, *2*, 2232–2236.

79. Michael, P.R.; Richmond, M.W.; Superfesky, M.J.; Stump, D.E.; Chavel, L.K. Potential of breakthroughs of impounded coal refuse slurry into underground mines. In Proceedings of the Environmental and Engineering Geoscience, Keystone, CO, USA, 11–15 April 2010; Volume 16, pp. 299–314.

80. Kang, J.; Sowers, T.D.; Duckworth, O.W.; Amoozegar, A.; Heitman, J.L.; McLaughlin, R.A. Turbidimetric Determination of Anionic Polyacrylamide in Low Carbon Soil Extracts. *J. Environ. Qual.* **2013**, *42*, 1902–1907. [CrossRef]

81. Azam, S. Large Strain Settling Behavior of Polymer-Amended Laterite Slurries. *Int. J. Geomech.* **2011**, *11*, 105–112. [CrossRef]

82. Hu, L.; Wu, H.; Zhang, L.; Zhang, P.; Wen, Q. Geotechnical Properties of Mine Tailings. *J. Mater. Civ. Eng.* **2017**, *29*, 04016220. [CrossRef]

83. Geremew, A.M.; Yanful, E.K. Dynamic Properties and Influence of Clay Mineralogy Types on the Cyclic Strength of Mine Tailings. *Int. J. Geomech.* **2013**, *13*, 441–453. [CrossRef]

84. Das, B.M. *Advanced Soil Mechanics*, 4th ed.; CRC Press; Taylor and Francis Group: Boca Raton, FL, USA, 2013; ISBN 9781482234831.

85. Yu, H. *Geotechnical Properties and Flow Behavior of Coal Refuse Under Static and Impact Loading*; Case Western Reserve University: Cleveland, OH, USA, 2015.

86. Beveridge, A.; Mutz, P.; Reid, D. Tailings co-disposal case study—Art or science? In Proceedings of the Paste 2015: Proceedings of the 18th International Seminar on Paste and Thickened Tailings, Cairns, Australia, 5–7 May 2015; pp. 505–520. [CrossRef]

87. Chiapponi, L. Water retention curves of multicomponent mixtures of spherical particles. *Powder Technol.* **2017**, *320*, 646–655. [CrossRef]

88. Rai, R.K.; Singh, V.P.; Upadhyay, A. *Chapter 17—Soil Analysis*; Academic Press: Cambridge, MA, USA, 2017; pp. 505–523, ISBN 978-0-12-811748-4.